

A Study of Flux Vortices in Type II Superconductors

Tim Blasius

2008 NSF/REU Program
Physics Department, University of Notre Dame

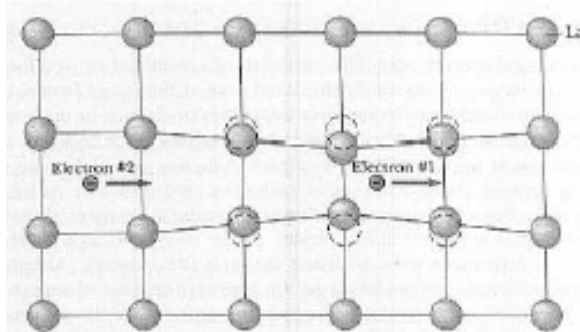
Advisor: Professor Morten Eskildsen

Abstract:

Superconductivity, while almost a hundred years old, is a physical phenomenon which yet retains important unexplained properties. In particular, the mechanism of high temperature superconductivity is poorly understood. This project focused on so-called type II superconductors. These materials, when subjected to an appropriate temperature and magnetic field, are characterized by the complete lack of electrical resistance and the confinement of magnetic flux to quantized vortex regions. These magnetic flux vortices repel each other and thus arrange themselves in a regular lattice called a flux line lattice. In this project we study the form of these flux line lattices to learn more about the material in question and the superconducting state. The magnetic vortices were studied by analyzing neutron diffraction patterns. Using the techniques of small-angle neutron scattering (SANS) and Fourier analysis, the magnetic field distribution in the sample can be inferred from the scattered intensity pattern on a detector.

Introduction to Superconductivity:

Heike Kamerlingh Onnes was the first to discover superconductivity in 1911 shortly after he successfully liquefied helium in 1908. It took nearly half a century before Bardeen, Cooper, and Schrieffer finally gave the scientific community a microscopic theory of superconductivity (BCS theory). One of the main qualitative ideas behind their theory is the creation of Cooper pairs of electrons. At low enough temperatures, electrons can actually attract one another, forming bound pairs by the exchange of sound quanta in a material's lattice. In other words, although in free space electrons will always repel each other, a material's lattice can actually create a negative permittivity leading to attraction. Qualitatively the process is as follows, as one electron travels through the lattice it will distort the positions of the positively charged lattice around it, creating a higher density of positive charge in its wake. This more densely packed region will then pull a trailing electron towards it and the two electrons can carry on in this fashion and are thus bound together with the lattice as a medium. This situation is displayed in the following illustration.



An energy gap is created by the binding of electrons in pairs. This energy gap leads to the electrons being unable to accept arbitrarily small amounts of energy from the lattice and thus they can travel without resistance.

BCS theory seemed a reasonable theoretical explanation of the superconducting state until, in 1986, Bednorz and Müller discovered high temperature superconductivity in cuprates. BCS appeared to predict a maximum critical temperature around 30K but the new high temperature cuprates have critical temperatures above 130K. This has led scientists to suspect that a mechanism other than phonon-exchange causes the pairing of electrons. Being given that BCS's microscopic description of superconductivity appears to fail with the cuprates, we are perhaps better served by understanding a phenomenological description of the superconducting state. The major phenomenological properties of type I superconductivity including perfect conductivity and the Meissner effect are given by the London equations:

$$1. \vec{E} = \frac{\partial}{\partial t} (\Lambda \vec{J}_s) \quad 2. \vec{B} = -c \cdot \nabla \times \Lambda \vec{J}_s \quad 3. \Lambda = \frac{4\pi\lambda^2}{c^2} = \frac{m^2}{n_s e^2}$$

The first equation speaks to perfect conductivity. It

states that an electric field will accelerate charged particles indefinitely, which is in contrast to Ohm's Law ($\vec{J} = \sigma \vec{E}$).

Now if we take equation 2 along with Maxwell's equation: $\nabla \times \vec{B} = \frac{4\pi\vec{J}}{c}$ using the curl operator and a vector product

identity, we get: $\nabla^2 \vec{B} = -\frac{4\pi\vec{J}}{c}$. This equation implies that the magnetic field is exponentially screened from the bulk of

the superconductor, a.k.a. the Meissner effect.

This expulsion of a magnetic field from the bulk of a superconductor is more than a perfect expression of Faraday's law. If one places a magnetic field through a material in the normally conductive state and then cools that sample until it is superconducting, the B-field will still be expelled despite no changing flux. We know that B-fields store

energy $\left(\int \frac{B^2}{2\mu_0} dv \right)$ and thus the Meissner effect requires an input of energy. It is easily imaginable that if a B-field of a

large enough magnitude were applied to a sample this would make the superconducting state energetically unfavorable.

This is where type II superconductors vastly differ. According to Ginzburg-Landau theory, some materials can remain superconducting at much larger applied fields because total expulsion from the bulk does not occur. Rather the B-field is allowed to penetrate in quantized vortices. These flux vortices then repel each other according to the Lorentz force and therefore arrange themselves in a lattice. It is precisely these flux vortices that we shall be studying in this project.

These magnetic vortices are invisible to the human eye. They must be studied by their magnetic interactions. The technique we employed (SANS) involves scattering neutrons off of the flux line lattice. We observe, in our experiment, a diffraction pattern on a detector and it is our goal to infer the magnetic field distribution in our sample from this observed intensity pattern. In order to understand our experimental results we must be familiar with lattice diffraction.

Understanding Lattice Diffraction

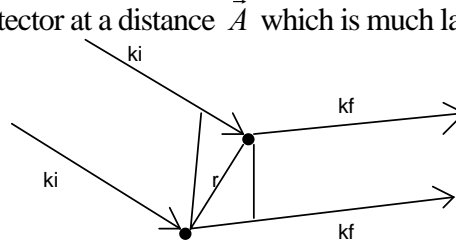
In this brief discussion of neutron diffraction through a lattice we will follow Stiddard¹. When we talk about lattice diffraction we are talking about passing a wave of neutrons through a regular array of vortices which act as scatterers of the wave. When we wish to describe and predict these intensity patterns it becomes important to remember the amplitude and the phase of the wave. We can represent the amplitude and phase of a wave with the following expression: $f(\vec{r}) = \phi_0 \exp(i(\vec{k}_0 \cdot \vec{r} - \omega t))$. If the amplitude of the scattered wave is measured at \vec{A} then we may write

$f(\vec{A}) = \frac{\phi_0 \alpha}{|\vec{A}|} \exp(ikA)$ where we have ignored the time dependence, added a factor α to describe the strength of the

scattering, and divided by A because we know that intensity is proportional to the norm square of f and also inversely proportionally to the distance squared. This implies that f is inversely proportional to the distance.

The previous discussion focused on one wave being scattered off of one scatterer at the origin and then being observed at a point \vec{A} . Now let us consider two waves being scattered, each off of a different vortex a distance \vec{r} apart.

We will observe the pattern on our detector at a distance \vec{A} which is much larger than the vortex separation.



Where $|k_i| = |k_f| = \frac{2\pi}{\lambda}$. Thus in this situation a phase difference is introduced. $\delta = \vec{r} \cdot \vec{k}_f - \vec{r} \cdot \vec{k}_i = \vec{r} \cdot (\vec{k}_f - \vec{k}_i)$.

Lets say $(\vec{k}_f - \vec{k}_i) = \vec{K}$. Now this additional phase difference must be introduced into our previous expression for phase

and amplitude of the wave. $f(\vec{A}) = \frac{\phi_0 \alpha}{A} \exp(ikA - i\vec{K} \cdot \vec{r})$ Now we can consider the total amplitude of the scattered

waves due to a system of N scatterers from the following expression:

$$f(\vec{A}) = \frac{\phi_0 \alpha}{A} \sum_{j=1}^N \exp(ikA - i\vec{K} \cdot \vec{r}_j) = \frac{\phi_0 \alpha}{A} \exp(ikA) \sum_{j=1}^N \exp(-i\vec{K} \cdot \vec{r}_j).$$

We could even consider a continuous distribution of scatterers (instead of discrete points) and we would turn the previous

sum into an integral: $F(\vec{K}) = \frac{\phi_0 \beta}{A} \exp(ikA) \int \rho(\vec{r}) \exp(-i\vec{K} \cdot \vec{r}) d\vec{r}$ where β is a constant which describes the

proportionality between the strength of scatterers, α , and $\rho(\vec{r}) d\vec{r}$. In our particular case, $\rho(\vec{r}) \propto B(\vec{r})$ and thus we

have: $F(\vec{K}) \propto \int B(\vec{r}) \exp(-i\vec{K} \cdot \vec{r}) d\vec{r}$. If we invert this expression we have: $B(\vec{r}) \propto \int F(\vec{K}) \exp(i\vec{K} \cdot \vec{r}) d\vec{K}$

Now let us consider the case where there is a scatterer at every lattice point, i.e. at every

$\vec{R} = \vec{r} = n_1 \vec{a}_1 + n_2 \vec{a}_2 + n_3 \vec{a}_3$, where $\vec{a}_1, \vec{a}_2, \vec{a}_3$ are basis vectors of the lattice, what would be the diffraction pattern on the

detector in this case? We are going to consider a parallel piped of dimensions $N_1\vec{a}_1, N_2\vec{a}_2, N_3\vec{a}_3$. An expression for the

$$\text{amplitude of scattered radiation is: } F_{\text{lattice}} \alpha \sum_{\vec{R}} \exp(-i\vec{K} \cdot \vec{R}) = \sum_{n_1=0}^{N_1-1} \sum_{n_2=0}^{N_2-1} \sum_{n_3=0}^{N_3-1} \exp[-i\vec{K} \cdot (n_1\vec{a}_1 + n_2\vec{a}_2 + n_3\vec{a}_3)]$$

$$\Rightarrow \sum_{n_1=0}^{N_1-1} \exp(-in_1(\vec{K} \cdot \vec{a}_1)) \sum_{n_2=0}^{N_2-1} \exp(-in_2(\vec{K} \cdot \vec{a}_2)) \sum_{n_3=0}^{N_3-1} \exp(-in_3(\vec{K} \cdot \vec{a}_3)) \alpha F_{\text{lattice}}$$

To better analyze this equation we are going to make use of the easy to manipulate geometric series:

$$\sum_{n=0}^{N_1-1} x^n = \sum_{n=0}^{\infty} x^n - \sum_{n=N}^{\infty} x^n = \frac{1}{1-x} - \frac{x^N}{1-x}$$

$$\text{Therefore: } \sum_{n=0}^{N_1-1} \exp(-in_1(\vec{K} \cdot \vec{a}_1)) = \frac{1 - \exp(-iN_1(\vec{K} \cdot \vec{a}_1))}{1 - \exp(-i(\vec{K} \cdot \vec{a}_1))} \quad F_{\text{lattice}} \text{ will be a product of three such terms. Then we}$$

are of course not interested directly in F_{lattice} but rather in $I \propto F_{\text{lattice}}^* \cdot F_{\text{lattice}}$. After careful algebraic manipulation

utilizing Euler's formula one arrives at the following result:

$$I = \frac{\sin^2\left(\frac{1}{2}N_1(\vec{K} \cdot \vec{a}_1)\right) \sin^2\left(\frac{1}{2}N_2(\vec{K} \cdot \vec{a}_2)\right) \sin^2\left(\frac{1}{2}N_3(\vec{K} \cdot \vec{a}_3)\right)}{\sin^2\left(\frac{1}{2}(\vec{K} \cdot \vec{a}_1)\right) \sin^2\left(\frac{1}{2}(\vec{K} \cdot \vec{a}_2)\right) \sin^2\left(\frac{1}{2}(\vec{K} \cdot \vec{a}_3)\right)}$$

This expression will only yield appreciable intensities when it is near its maximum which occurs when:

$$\vec{K} \cdot \vec{a}_1 = 2\pi \cdot l_1 \text{ and } \vec{K} \cdot \vec{a}_2 = 2\pi \cdot l_2 \text{ and } \vec{K} \cdot \vec{a}_3 = 2\pi \cdot l_3$$

Where l_1, l_2, l_3 are integers.

$$\Rightarrow n_1 \cdot \vec{K} \cdot \vec{a}_1 = 2\pi \cdot l_1 \cdot n_1 \text{ and } n_2 \cdot \vec{K} \cdot \vec{a}_2 = 2\pi \cdot l_2 \cdot n_2 \text{ and } n_3 \cdot \vec{K} \cdot \vec{a}_3 = 2\pi \cdot l_3 \cdot n_3$$

$$\Rightarrow \vec{K} \cdot (n_1\vec{a}_1 + n_2\vec{a}_2 + n_3\vec{a}_3) = \vec{K} \cdot \vec{R} = 2\pi \times \text{integer.}$$

Upon inspection, one can convince oneself, that the previous equation is satisfied if $\vec{K} = l_1\vec{b}_1 + l_2\vec{b}_2 + l_3\vec{b}_3$ where the b-

vectors are defined in the following manner:

$$\Rightarrow \vec{b}_1 = \frac{2\pi(\vec{a}_2 \times \vec{a}_3)}{\vec{a}_1 \cdot (\vec{a}_2 \times \vec{a}_3)} \quad \Rightarrow \vec{b}_2 = \frac{2\pi(\vec{a}_3 \times \vec{a}_1)}{\vec{a}_2 \cdot (\vec{a}_3 \times \vec{a}_1)} \quad \Rightarrow \vec{b}_3 = \frac{2\pi(\vec{a}_1 \times \vec{a}_2)}{\vec{a}_3 \cdot (\vec{a}_1 \times \vec{a}_2)}$$

These three vectors will also span a lattice, but not that of the crystal. Since the units of \vec{K} are (1/length) we shall call this lattice the reciprocal lattice. Linear integer combinations of these basis vectors of the reciprocal lattice point out

the locations of maximum intensity. In other words, the locations of appreciable intensity on our detector due to diffraction of radiation by a crystal lattice occur at the points of the reciprocal lattice.

Now that we know the intensity behaves as a three-dimensional Dirac delta function, we can rewrite the following relation $B(\vec{r}) \propto \int F(\vec{K}) \exp(i\vec{K} \cdot \vec{r}) d\vec{K}$ as a summation $B(\vec{r}) \propto \sum_{\vec{K}} F(\vec{K}) e^{i\vec{K} \cdot \vec{r}}$. We can further get rid of this

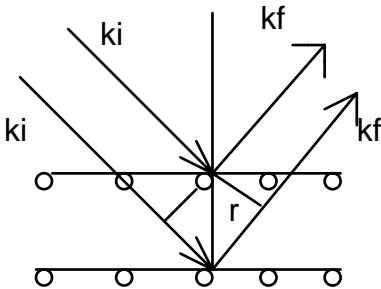
nebulous proportionality symbol by a thorough analysis of the scattering experiment. A thorough analysis yields

$$|F|^2 = R \frac{16 \cdot \phi_0^2 \cdot K}{2 \cdot \pi \cdot \gamma^2 \cdot \lambda_n^2 \cdot t} \cos(\eta)^2$$

In this equation R is the integrated intensity, ϕ_0 is the flux quantum, γ is the neutron's gyromagnetic ratio, λ_n is the wavelength of the neutrons, t is the thickness of the sample, and η is the polar angle of the peak on the detector. Using these form factors we can compute an approximation of the previous summation with the first few terms and thus we can approximate real-space magnetic field distribution in the sample.

Equivalence with Bragg's Law

The preceding analysis was long and cumbersome at times. Fortunately there is an easier way to understand crystal diffraction. Bragg's law tells that we can consider a lattice of atoms to be a series of parallel planes. The places where the intensity is greatest becomes where constructive interference occurs between radiation reflecting off of different lattice planes. The path difference must be a constant multiple of the wavelength: $n\lambda = 2d \sin(\theta)$.



Where theta is the angle from the vertical and the magnitude of r is d . If the path difference needs to be a multiple of the wavelength then the phase difference needs to be a constant multiple of 2π .

$$\Rightarrow \vec{r} \cdot (\vec{k}_f - \vec{k}_i) = \vec{r} \cdot \vec{K} = n \cdot 2\pi$$

Now \vec{r} is a vector that connects two of the lattice points and thus can be seen as one of the vectors of the form: $n_1 \vec{a}_1 + n_2 \vec{a}_2 + n_3 \vec{a}_3$. Since Bragg's Law should hold

$$\text{for any set of points in any plane, in general Bragg's Law states: } \vec{R} \cdot \vec{K} = 2\pi \times \text{integer} \Rightarrow \vec{K} = l_1 \vec{b}_1 + l_2 \vec{b}_2 + l_3 \vec{b}_3$$

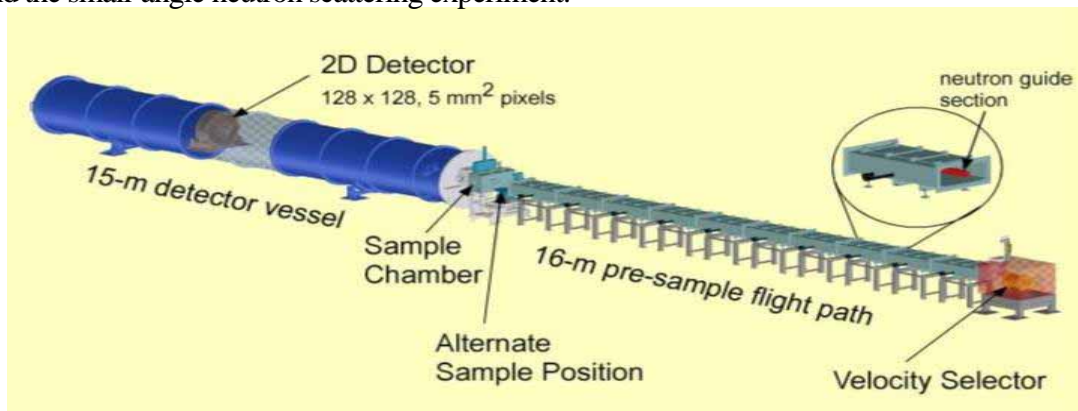
And Thus Bragg's Law agrees with the preceding analysis; the intensity pattern is greatest at points corresponding to the reciprocal lattice.

Bragg's Law is significantly simpler to think about. It tells us that there will be a maximum of intensity on our detector only when the incident intensity makes a certain angle with the lattice planes. One could imagine rotating a

sample so that the intensity on the detector would start at a minimum, move through the point where it satisfied the Bragg condition reaching a maximum, and then go back down to a minimum again. This procedure creates a so-called “rocking curve” of intensity and it is exactly what was done in our experiment.

Experiment

Now that we understand the basic tenants of superconductivity and lattice diffraction we are ready to understand the small-angle neutron scattering experiment.



This is a diagram of the SANS set-up at NIST (National Institute of Standards and Technology).³ The reactor allows neutrons with wavelength 5-20 angstroms to travel down the beam line.⁴ To select a particular wavelength there is a velocity selector which consists of a drum with curved grooves on it. This drum spins and if the neutrons are traveling with just the right speed then they will make it through the slits and continue down the neutron guides.

The neutron guides work in a manner analogous to fiber optic cables. In fiber optic cables, the index of refraction is such that light is totally internally reflected all the way down the wire and thus not allowed to escape. The neutrons in the neutron guide behave in a similar fashion.

Next the neutrons pass through a collimation slit at a distance of around 13 meters from the sample chamber and then another aperture directly in front of the sample. These serve to reduce the angular spread of the incident neutron beam and focus it on the sample.

Then the beam arrives at the cryomagnet. Our sample was the type II superconductor $(\text{Ba,K})\text{Fe}_2\text{As}_2$ which has a T_c of about 30 K.⁵ We worked, however, at the instrument's base temperature of 2.7 K. This required lowering our sample to the bottom of a cryomagnet, filling an outer layer with liquid nitrogen and then an inner layer with liquid helium.

Next it is necessary to apply a magnetic field to our sample so that a superconducting vortex state will evolve. With this substance H_{c1} is a few mT and H_{c2} is estimated at 100 T.⁵ We applied fields from .025 T to 1 T. To do this we

used a superconducting magnet. The leads across the superconducting magnet were heated so that it became normally conductive and then when the appropriate current was achieved, it was cooled again so that the whole magnet would be superconducting with no energy losses.

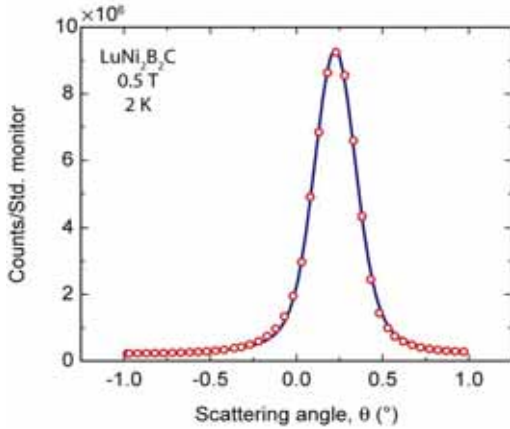
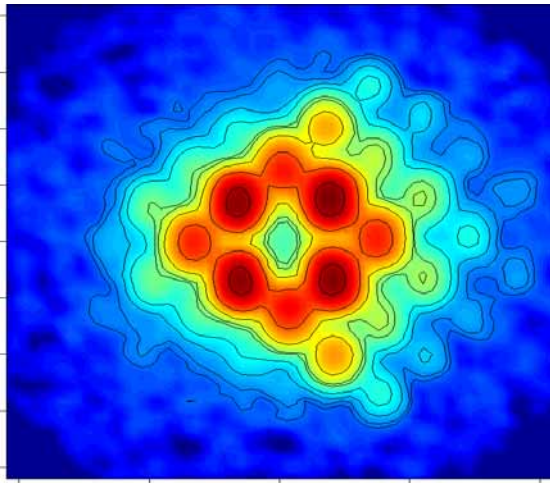
After the sample has been set-up appropriately, the incoming neutrons will scatter off of the vortices. They will be deflected by a small angle and then allowed to travel about 15 meters down an evacuated chamber before colliding with a detector.⁴ This long length is used so that a small angular deflection can turn into an appreciable displacement on the detector. A beamstop is put in place so that the detector is not fried by the large intensity of the center of the beam, which is largely un-deflected. A ³He position-sensitive proportional counter relays the information about where on the detector the neutrons strike.⁴ This then allows us to analyze the intensity pattern.

From our discussion of Bragg's law, we know that the intensity peaks only arise when the incoming radiation strikes the crystal planes at a certain angle. This makes it prudent to rotate our sample in the beam so that the radiation will strike at a myriad of different angles thus exciting different intensity peaks. It is for this reason that a typical experimental run involves a scan where the sample is rotated in small steps, for a total of a few degrees, in the beam line.

Oftentimes, the intensity scattered into the peaks is not great enough to allow the peaks to be easily differentiated from the background. In this case, we can perform a background subtraction. To do this we simply need to make the vortices disappear and then observe how the material scatters neutrons. We accomplished this in two ways; raising the temperature of the material above the critical temperature or reducing the magnetic field to zero. The scans taken with these settings could then be subtracted from the scans with the vortices in place to make the peaks stand out more profoundly.

Now, for the particular sample (Ba,K)Fe₂As₂ we did not see any vortices in our experimental runs. However, I conducted further analysis on previous data, taken before my arrival. This data was on a sample of LuNi₂B₂C and the rest of the discussion of analysis in this paper will be based on this data.

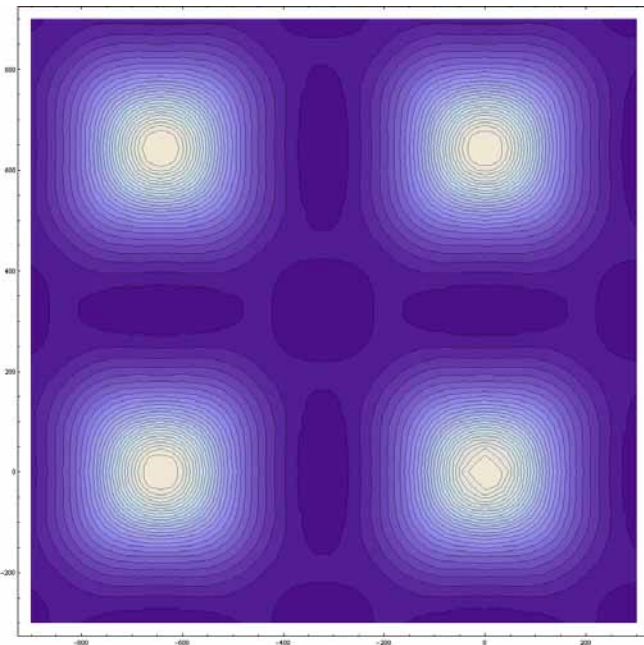
Analysis



rocking curve of intensity pictured above. The area under this curve is then the integrated intensity used in the form factor. Once we have all of this information, we can determine the form factors for several of the peaks in the intensity

pattern and then approximate the following sum: $B(\vec{r}) = \sum_{\vec{K}} F(\vec{K})e^{i\vec{K}\cdot\vec{r}}$, which allows us to do a real-space

reconstruction of the B-field. An example contour plot for a unit cell of the magnetic field in LuNi₂B₂C looks as follows:



We can be reasonably assured that this is an accurate reconstruction, even though we did not include all the terms in the sum, because we notice subsequent terms yield increasingly insignificant corrections.

Conclusion

We have thus completed what we had set out to do. Qualitatively speaking our task was not difficult to understand. We simply desired to observe the magnetic flux vortices we believed would be there from energy considerations and Ginzburg-Landau theory. The vortices are not phenomenon visible to the naked eye, and so we decided to view them via their magnetic interactions with a beam of neutrons. We sought to backwards infer the magnetic field distribution in the sample based on an intensity pattern of scattered neutrons. This required us to understand lattice diffraction and resulted in an expression for the B-field involving an arbitrarily large sum. This sum was then well-approximated by keeping only the first few terms concerning the brightest intensity peaks.

The B-field reconstruction and the form factors that constitute it are very important in the field of superconductivity. Numerous theories have surfaced which offer to explain properties of the superconductive state for high-temperature type II superconductors. These theories make predictions about the magnitude of the form factors. Our data can be used to check the accuracy of these theories' predictions. Data such as ours can be used to nudge theorists in the correct direction for a successful explanation of type II superconductors.

My future research with this group will involve continued experimentation on the new Iron Arsenic superconductor, $(\text{Ba,K})\text{Fe}_2\text{As}_2$. We will be traveling to the neutron source at the Institut Laue-Langevin (ILL) in Grenoble, France in early September. The neutron beam at ILL can attain intensities several times greater than that of the neutron beam at NIST. We are hopeful that this greater intensity in the incident beam will allow the diffraction peaks to stand out better from the background. I look forward to studying again the flux line lattice structure of this type II superconductor.

I would like to thank Notre Dame University and by extension the National Science Foundation for funding my research endeavors this summer. I would also like to thank Professor Eskildsen for teaching me everything I now know about superconductors and Professor Garg for obtaining supplementary funding for me. Finally, I appreciate the efforts of Pinaki Das, John Densmore, Cornelius Griggs, and Lisa DeBeer-Schmitt in helping me to learn the ropes of analysis and the experimental process.

Bibliography

- 1 Stiddard, *The Elementary Language of Solid State Physics*, Academic Press, London (1975)
- 2 Morten Ring Eskildsen, Ph.D. thesis, Risø National Laboratory, Roskilde, Denmark, 1998
- 3 Image taken from: <http://www.ncnr.nist.gov/instruments/ng7sans/>
- 4 Information taken from this website: <http://www.ncnr.nist.gov/instruments/ng7sans/instrumentSpecs.html>
- 5 N. Ni, S. L. Bud'ko, A. Kreyssig, S. Nandi, G. E. Rustan, A. I. Goldman, S. Gupta, J. D. Corbett, A. Kracher, P. C. Canfield, *Anisotropic thermodynamic and transport properties of single crystalline $(Ba_{1-x}K_x)Fe_2As_2$ ($x = 0$ and 0.45)*, <http://xxx.lanl.gov/archive/cond-mat> , 11 Jun 2008